J. Biochem. **133**, 693–698 (2003)
DOI: 10.1093/jb/mvg089

Neutralization of Toxic Heme by *Plasmodium Falciparum* Histidine-Rich Protein 2

Nguyen Tien Huy, Satoshi Serada, Dai Thi Xuan Trang, Ryo Takano, Yoshiro Kondo, Kenji Kanaori, Kunihiko Tajima, Saburo Hara and Kaeko Kamei*

Department of Applied Biology, Kyoto Institute of Technology, Matsugasaki, Sakyo-ku, Kyoto 606-8585

Received February 20, 2003; accepted March 13, 2003

***Plasmodium falciparum* histidine-rich protein 2 (PfHRP2) has been suggested to be an initiator of the polymerization of heme, which is produced as by-product on the digestion of hemoglobin, and a promoter of the H_2O_2-induced degradation of heme in food vacuoles of the malarial parasite. In this work, we have designed PfHRP2 model peptides, R18 and R27 (18 and 27 residues, respectively), and used them for optical and electron spin resonance spectroscopic measurements to confirm that the axial ligands of the heme-PfHRP2 complex are the nitrogenous donors derived from the imidazole moieties of histidine residues of PfHRP2. In addition, we revealed that the affinities of R18 and R27 for heme (K_d = 2.21 × 10^{-6} M and 0.71 × 10^{-6} M, respectively) might be as high as that of PfHRP2 (K_d = 0.94 × 10^{-6} M). The R27 peptide can remove heme from membrane-intercalated heme and inhibit heme-induced hemolysis. Therefore, we suggest another function of PfHRP2: it may play an important role in the neutralization of toxic heme in the parasite cytoplasm and infected erythrocytes by removing heme from heme-bound membranes or reducing heme-induced hemolysis.**

Key words: heme, hemolysis, histidine-rich protein, malaria, membrane damage.

Abbreviations: DMSO, dimethylsulfoxide; EDT, 1,2-ethanedithiol; ESR, electron spin resonance; Fmoc, 9-fluorenylmethyloxycarbonyl; HEPES, 2-[4-(2-hydroxyethyl)-1-piperazinyl]ethanesulfonic acid; HOBt, 1-hydroxybenzotriazole; PfHRP, *Plasmodium falciparum* histidine-rich protein; *t*-Bu, *tert*-butyl; TFA, trifluoroacetic acid; Trt, trytyl. We defined ferric protoporphyrin IX as heme or protoheme, and ferric mesoprotoporphyrin IX as mesoheme.

Malaria is one of the most common diseases in tropical countries. Each year, there are 300 million new malarial cases and millions of deaths due to malaria all over the world. The fast spreading resistance to current quinoline antimalarials has made malaria a major global disease (*1*). Artemisinin-resistant strains of *Plasmodium falciparum* have also been developed in the laboratory (*2*). Therefore, it is necessary to clearly understand the pathology of malaria and investigate new antimalarials for curing patients.

During the intra-erythrocytic stage of malaria, since hemoglobin is utilized as a major source of amino acids by the malarial parasite, free heme is released inside the malarial compartment. The released heme, which is extremely hazardous to the cell membrane, changes the homeostasis of the malarial cell, and binds to some malarial enzymes and inhibits their activities, causing malarial death (*3–6*). The malarial parasite detoxifies heme through the specific mechanism of heme polymerization (*7*), or degradation of heme by H_2O_2 in food vacuoles (*8*, *9*) and by reduced glutathione in the parasite cytoplasm (*10–12*).

P. falciparum histidine-rich protein 2 (PfHRP2), which is composed of repeats comprising three amino acids: histidine (34%), alanine (37%), and aspartic acid (10%) (*13*), is synthesized by the parasite in the parasite compartment and excreted from erythrocytes as a water-soluble protein (*14*). PfHRP2 is also delivered to the parasite's food vacuoles, in which PfHRP2 initiates the polymerization of heme (*15*) and promotes H_2O_2-induced degradation of heme at pH 5.2 (*9*). However, the function of PfHRP2 in the parasite cytosol and erythrocytes as well as in the host plasma remains equivocal. In this work, we designed mimic peptides based on the repetitive sequence of PfHRP2, and studied the role of PfHRP2 in the protection of parasite and erythrocyte membranes from toxic heme using the mimic peptides and erythrocyte membranes.

MATERIALS AND METHODS

Materials—Hemin (heme) was purchased from Sigma. Human blood was obtained from healthy volunteers. Dimethyl sulfoxide (DMSO) was from Wako Pure Chemicals, Osaka. Fmoc-amino acids were obtained from Peptide Institute (Osaka). All other chemicals were of the best available grade.

Peptides Synthesis—Two peptides, with the following sequences, were synthesized:

18R, Ala-His-His-Ala-His-His-Ala-Ala-Asp-Ala-His-His-Ala-His-His-Ala-Ala-Asp (two repeats of Ala-His-His-Ala-His-His-Ala-Ala-Asp);

27R, Ala-His-His-Ala-His-His-Ala-Ala-Asp-Ala-His-His-Ala-His-His-Ala-Ala-Asp-Ala-His-His-Ala-His-His-Ala-Ala-Asp (three repeats of Ala-His-His-Ala-His-His-Ala-Ala-Asp).

*To whom correspondence should be addressed. Tel: +81-75-724-7553, Fax: +81-75-724-7532, E-mail: kame@ipc.kit.ac.jp

The peptides were synthesized by means of the solid-phase procedure using TGS-PHB-Asp(*t*-Bu)-resin, Fmoc-amino acids and an automatic peptide synthesizer (model PSSM-8; Shimadzu, Kyoto). All the deblocking, rinsing, and coupling steps were carried out according to the manual of the manufacturer. Temporary protection of the side chain groups of His and Asp was accomplished with Trt and *t*-Bu groups, respectively. Coupling was performed with HOBt active esters. After synthesis, each peptide was cleaved from the resin with 94% TFA containing 5% anisole and 1% EDT at room temperature for 2 h. The peptide was recovered as a precipitate with diethyl ether. The synthesized peptide was purified by reversed phase chromatography on an Inertsil ODS-3 (4.6 × 250 mm; GL Science, Tokyo) column by HPLC. The column was equilibrated with 0.1% TFA and eluted with an 80-min linear gradient of 0 to 80% acetonitrile containing 0.1% TFA. The flow rate was 1 ml/min and the peptide was monitored as the absorbance at 230 nm. Each peptide was obtained as a single peak after repetitive chromatographies under the same conditions as described above. The molecular masses of the purified peptides were determined in the positive mode with a laser ionization TOF mass spectrometer (KOMPACT MALDI II; Kratos Analytical, Manchester, UK). The amino acid compositions and peptide concentrations were determined with an amino acid analyzer (model L-8500A; Hitachi, Tokyo) after hydrolysis with 6 N HCl at 110°C for 24 h in vacuo. The results of mass spectrometry and amino acid analyses of the peptides were identical with those expected.

Hemin Preparation—A stock heme solution was prepared freshly by dissolving hemin chloride in 20 mM NaOH, followed by centrifugation for 10 min at 15,000 rpm to remove remaining hemin crystals. Heme concentrations were determined from the absorbance at 385 nm in NaOH and ε_{mM} = 58,400 (*16*). This stock solution (1 mM) was kept in the dark on ice and used within 24 h.

Absorption Spectra—All absorption spectra were recorded with a Hitachi U-3300 double beam spectrophotometer (Tokyo) using 1.0-cm light path quartz cuvettes at 25°C. The conditions for measurements are given in the figure legends.

Spectrometric Titration—Optical absorption spectra were also recorded with a Hitachi U-3300 double beam spectrophotometer, as described in our previous report (*17*). Briefly, the binding of peptides to heme was titrated by adding increasing amounts of the peptides (0–110 μM for R18 and 0–22 μM for R27) in a sample cuvette containing 10 μM heme in 100 mM phosphate buffer (pH 7.4), the reference cuvette containing phosphate buffer only. In the present study, we used the increase in absorbance at 413 nm to monitor the formation of the heme-peptide complex. Heme binding curves were constructed by plotting ΔA_{413} *versus* the peptides concentration. The heme binding curves were fitted to the following equilibrium binding equation (*18*).

$$RL^* = [(L_t^* + R_t + K_d) - [(L_t^* + R_t + K_d)^2 - 4R_tL_t^*]^{1/2}]/2 \quad (1)$$

Where L^* is the free ligand concentration, R_t the total receptor concentration (heme concentration), L_t^* the total ligand concentration, and K_d the dissociation affinity constant of the heme-ligand complex.

ESR Measurement of Heme-Peptide Complexes—Heme-peptide complexes were prepared by incubation of 0.5 mM mesoheme and 0.5 mM R27 or R18 in 100 mM phosphate buffer (pH 7.4) containing 2.86% DMSO for 1 h at room temperature. The complexes formed were monitored with a JES-TE 300 ESR spectrometer (JEOL, Tokyo) at 4.2 K with 100 kHz field modulation. The frequency counter included in the spectrometer was monitored as the microwave frequency of each measurement. The magnetic field strength was calibrated by hyperfine splitting of the Mn (II) ion (8.69 mT) doped in MgO powder. Powdered lithium-tetracyanoquinodimethane radical (Li-TCNQ, g = 2.0025) was used for the standard g-value. The ESR data were analyzed and calibrated using a Winrad system (Radical Research, Tokyo). The typical conditions for ESR measurements were as follows: microwave power, 6.0 mW; modulation magnitude, 0.68 mT; sweep range, 30 mT to 500 mT; sweep time, 4 min; and time constant, 0.1 s.

Effects of Peptides on Heme-Induced Hemolysis—Fresh blood from healthy volunteers was heparinized (1 mg heparin/ml of blood) to prevent clotting and used within 48 h. In this manner, no more than 2.5% hemolysis occurred in controls when no hemin was added. Erythrocytes were separated from plasma by centrifugation at 1,500 ×*g* for 3 min and washed six times with an isotonic standard buffer (50 mM sodium phosphate buffer containing 68 mM NaCl, 4.8 mM KCl, and 1.2 mM $MgSO_4$, pH 7.4) (*19*, *20*). Thereafter, the effects of R27 and R18 on the heme-dependent hemolysis were studied using 0.5% cell suspensions in the isotonic buffer. Suspensions (0.6 ml) of 0.5% erythrocytes were shaken at 140 cycles/min with 20 μM heme in absence or presence of R27 or R18 (0, 0.5, 2, 5, 10 or 20 μM) at 37°C for 150 min. Intact erythrocytes were then removed by centrifugation at 1,500 ×*g* for 3 min, and the amount of hemoglobin released from the hemolyzed erythrocytes into the supernatant was determined by measuring the absorbance at 578 nm (*21*). The pelleted intact erythrocytes were lysed with water and then centrifuged to obtain a supernatant, the hemoglobin content of intact erythrocytes being also measured using the absorbance at 578 nm. The degree of hemolysis was calculated from the ratio of the hemoglobin content released from erythrocytes hemolyzed by heme to the total heme content of the erythrocytes (*21*).

Preparation of Human Erythrocyte White Ghost Membranes—Washed erythrocytes (2.5 ml) were hemolyzed in 35 ml of phosphate buffer (5 mM, pH 8.0). After vigorous shaking, the hemolysate was centrifuged for 20 min at 35,000 ×*g*. The supernatant was removed by aspiration. This step was repeated. The membranes were washed many times with 50 ml of Tris-HCl (pH 7.4) until the pellet became white. The membranes were finally resuspended in 2.5 ml of the same buffer. At each centrifugation step, the brown-colored button that formed on the bottom of the membrane fraction was removed carefully (this button is supposed to be proteinase). All steps were carried out on ice. The membranes were stored on ice and used within 24 h after preparation. The concentration of membrane protein was determined with a Bio-Rad Pro-

Table 1. **Electronic absorption maxima and ESR parameters of heme-peptides and related ferric low-spin complexes.**

Sample	Solvent	Absorption maxima (nm)			g_1	g_2	g_3	$\|R/\mu\|$*	$\|\mu/\lambda\|$*	Reference
Heme-R18	Phosphate buffer[a]	413	533	564	2.95	2.26	1.50	0.57	3.25	This study
Heme-R27	Phosphate buffer[a]	413	533	563	2.95	2.26	1.50	0.57	3.25	This study
Heme-imidazole	40% DMSO[a]	410	535	560	2.98	2.24	1.48	0.54	3.41	This study
Heme-*N*-methylimidazole	Phosphate buffer[a]	413	535	564	–	–	–	–	–	(*24*)
Heme- PfHRP2	Hepes buffer[b]	415	538	566	2.94	2.26	1.62	0.52	3.89	(*25*)
Cyt b-559 from maize[b]	Phosphate buffer[a]	–	–	–	2.94	2.27	1.54	0.570	3.364	(*24*)

[a]At pH 7.4; [b]At pH 7.0; *Calculated using Bohan's proposal (*27*).

tein Assay Kit (Bio-Rad, USA) using bovine serum albumin as a standard.

Effects of Peptides on Binding of Heme and Erythrocyte White Ghost Membranes—Prior to experiments, heme-R18 and heme-R27 complexes were formed by mixing heme with R18 and R27, respectively, in 0.2 M HEPES, pH 7.4. Suspensions of white ghost membranes containing 20 μg membrane protein were incubated with 5 μM heme, heme-R18 complex (mixture of 5 μM heme and 5 μM R18), or heme-R27 (mixture of 5 μM heme and 5 μM R27) in 0.6 ml of 0.2 M HEPES, pH 7.4, for 7 min at room temperature. Then the membranes were collected as pellets by centrifugation at 15,000 rpm for 10 min, and washed twice with the same buffer. The amounts of heme bound to erythrocyte membranes were determined with a spectrophotometer (Hitachi U-3300) at 402 nm after solubilization of the membrane pellet in 2.5% SDS buffered with 50 mM Tris-HCl, pH 7.4. The concentrations of heme and heme-peptide complexes were calculated from calibration curves for pure heme and heme-peptide complexes, respectively, which had been obtained before addition to the membrane ghosts. The amount of heme associated with the membranes is expressed as nmol heme per mg membrane protein.

Removal of Heme from Heme-Membrane Complexes by Peptide R27—In preliminary experiments, the amounts of heme bound to membranes were determined after incubation of a mixture of white ghost membranes and heme for various periods. The results demonstrated that 7-min incubation was enough for heme to bind with membranes and no further heme bound to the membranes. Thus, we determined the optimum experimental conditions as follows.

Suspensions of white ghost membranes containing 150 μg membrane protein were incubated with 30 μM heme in 1 ml of Tris-HCl buffer (50 mM, pH 7.4) for 7 min at room temperature. After incubation, the membranes were washed three times with the same buffer until all residual heme had been removed. Membranes binding heme were resuspended in 1 ml of the same buffer, divided into three tubes (each containing 0.3 ml of a sample), and incubated with 20 μM R18, 20 μM R27 or the buffer as a control. After incubation at room temperature for 30 min, the mixtures containing membranes were separated into pellets and supernatants by centrifugation (15,000 rpm, 10 min). Then the pellets were dissolved in 0.3 ml of 50 mM Tris-HCl (pH 7.4) containing 2.5% SDS. The amount of heme remaining in the membranes was determined as the absorbance recorded with a Hitachi U-3300 double beam. The amounts of heme released by peptides from membranes into supernatants were also determined.

RESULTS AND DISCUSSION

Absorption Spectra of Heme Complexed with Peptides—The absorption spectrum of heme (10 μM) in phosphate buffer (100 mM, pH 7.4) shows Soret and Q bands absorption at 385, 493, and 616 nm (data not shown), which are characteristic of the high-spin complex taking the five coordinate structure (*22*, *23*) with a weak axial ligand such as water or a chloride anion. When excess R18 (final concentration, 110 μM) was added to the mixture, the Soret band shifted towards red at 413 nm, and Q band absorption was evident at 533 and 564 nm, as summarized in Table 1. The observed spectrum was classified as a six coordinate complex having strong ligands at both axial positions. In fact, the spectroscopic properties of heme and excess R27 (22 μM) (Soret, 413 nm; Q bands, 533 and 563 nm) coincided with those of similar solutions, as shown in Table 1. Furthermore, heme-bis-imidazole complexes exhibit similar spectra (*24*, *25*), as summarized in Table 1. These results supported the concept that R18 and R27 exhibit affinities for the heme chromophore.

ESR Spectra of Heme-Peptide Complexes—We further confirmed the electronic and coordination structures of heme-peptide complexes by electron spin resonance spectroscopy (ESR). Before the addition of R27, the observed ESR spectrum (figure not shown) of mesoheme (0.5 mM) exhibited an axial symmetric line shape ($g_\perp$ = 6 and $g_{//}$ = 2.0), which is typical of the ferric high-spin (S = 5/2) species, having a five coordination geometry (*26*). Upon adding R27 (final concentration, 0.5 mM) to the reaction mixture, the ESR signal intensities of the high-spin species significantly decreased with the concomitant formation of a new paramagnetic species with a distorted rhombic ESR line (g_1 = 2.97, g_2 = 2.24, and g_3 = 1.47), which is characteristic of ferric low-spin complexes (S = 1/2) having strong axial ligands at both axial positions. Similar results were obtained on measurement of the heme-R18 complex. The observed ESR spectrum of the low-spin species was quite similar to that recorded for a frozen mixture of the heme-PfHRP2 complex (*25*). In addition, the observed g-values of these complexes agreed well with each other [*e.g.*, heme-imidazole and heme-PfHRP2 complexes] (Table 1). The crystal field parameters, rhombicity $|R/\mu|$ and tetragonality $|\mu/\lambda|$ of the heme-peptide complexes and related complexes were calculated in terms of Bohan's proposal (*27*). The calculated crystal field parameters of heme-peptide complexes accorded well with those of heme-imidazole complexes, as summarized in Table 1. On the bases of the results obtained on ESR and optical measurements, as well as with the crystal field calculation, we concluded that the axial ligands

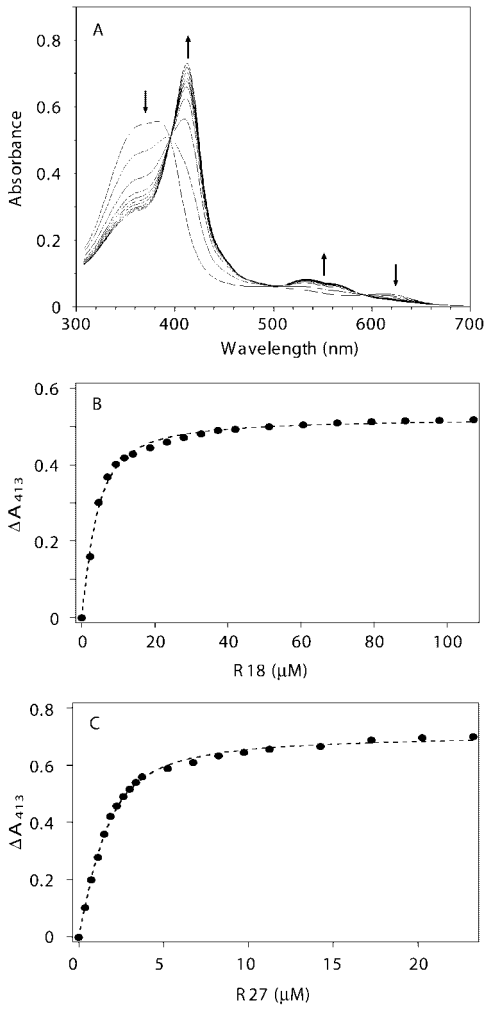

Fig. 1. **Titration of the heme-peptide interaction. Differential spectral titration of peptides with 10 μM heme was performed as described in the text.** The concentration of R18 (A) was increased from 0 μM to 110 μM, and that of R27 from 0 μM to 22 μM. Arrows indicate the effects of increasing concentrations of R18. Heme-binding curves generated from the difference absorption spectra by plotting ΔA_{413} *vs.* the R18 (B) or R27 (C) concentration. Eq. 1 given in the method section was used to fit the curves (dot lines).

of a heme-peptide complex are, therefore, the nitrogenous donors derived from the imidazole moieties of histidine residues of the peptide.

Spectrophotometric Heme Titration with Peptides—To evaluate the binding affinities of these peptides to heme, optical absorption spectra were measured with a spectrophotometer. As depicted in Fig. 1A, the heme solution gave broad Soret- and Q-band absorption maxima at 385 and 616 nm, respectively. As summarized in Table 1, on addition of 18R to the solution, the Soret band absorption maximum was red shifted to 413 nm, and the absorption coefficient showed a concomitant increase depending on the concentration of 18R. In contrast, the Q-band absorption maxima showed a characteristic blue-shift to 533 nm and 564 nm. The observed spectral change demonstrated the formation of the heme-18R complex. The three isobestic points, 395 nm, 501 nm and 595 nm, were experimental support that two absorbing species, heme and the heme-18R complex, were present in the reaction mixture. A similar spectral change was observed when 27R was titrated against heme (data not shown).

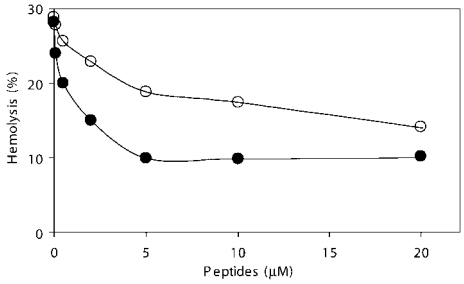

Fig. 2. **Effects of peptides on heme-induced hemolysis.** Suspensions of erythrocytes were incubated for 5 min with 20 μM heme without or with 0, 0.5. 2, 5, 10 or 20 μM R18 (open symbols) or R27 (closed symbols), and then shaken at 140 cycles/min for a further 150 min. Thereafter, the degree of hemolysis was measured.

Heme-binding curves, constructed by plotting ΔA_{413} versus the peptides concentration, are shown in Fig. 1, B and C. The plots obtained with heme binding curves were well coincident with respect to nonlinear least squares fitting to Eq. 1 for both R18 and R27. This fitting also yielded equilibrium dissociation constants $K_d = 2.21 \times 10^{-6}$ M and 0.71×10^{-6} M for heme-R18 and heme-R27, respectively. The K_d values were reproducible. On comparison of these K_d values with that of the heme-PfHRP2 complex, 0.94×10^{-6} M (*25*), R27 was found to bind to heme as strongly as PfHRP2 does, while R18 exhibited lower affinity for binding heme.

Furthermore, the relative affinity of these peptides for heme, i.e. their ability to compete for heme with bovine serum albumin (BSA), which forms a complex with heme with a K_d of about 10 nM (*28*), was examined. As expected from the relative K_d values, neither of the two peptides (at molar equivalent) is an effective competitor with BSA for heme (data not shown).

Effects of Peptides on Heme-Induced Hemolysis—Although R18 and R27 can not compete with BSA for heme, BSA having been reported to be able to inhibit heme-induced hemolysis (*29*), their roles in heme-binding under conditions of hemolysis remain to be evaluated. The hemolysis induced by heme was clearly inhibited by R18 as well as R27 (Fig. 2). This inhibition depended on the peptide concentration added. Also, R27 inhibited hemolysis more effectively than R18 does, perhaps due to its higher affinity to heme than that of R18.

To explain the effects of peptides on the heme-induced hemolysis, we compared the binding of heme alone and heme-peptide complexes to erythrocyte white ghost membranes. The results, as shown in Table 2, revealed that about 38% of the heme-binding to cell membranes was inhibited by formation of the complex with R27, while R18 only slightly affects the binding of heme and membranes. It is supposed that the hydrophobicity of heme is greatly reduced by binding histidine-rich peptides (R18 and R27). As a result, these complexes may exhibit lower affinity with membranes resulting in a lower amount of heme bound to the membranes (Table 2), reducing the level of heme-dependent hemolysis (Fig. 2).

Table 2. **Effects of R18 and R27 on binding of heme and white ghost membranes.**

Additives	Heme bound to membranes (nmol heme/mg protein)
5 μM heme	42.4 ± 3.0
5 μM heme + 5 μM R18	38.7 ± 1.7
5 μM heme + 5 μM R27	26.4 ± 1.4

We further investigated the effects of peptides on the heme-membrane complex. First, we prepared heme-bound membranes. After a peptide had been added and incubation, the membrane and supernatant were separated by centrifugation, and then the heme contents were determined by means of absorption spectra. In the case of the membrane fraction, the absorption spectrum was recorded after lysis of the membranes by SDS.

After incubation of heme-bound membranes with only the buffer, heme remaining in the membranes (spectrum 4 in Fig. 3) gave an absorption spectrum with a relatively sharp Soret-band, the Soret- and Q-band absorption being maximal at 400 nm, and 520 and 610 nm. The spectrum indicates that heme in membranes exists as high-spin complex with a weak axial ligand such as water or a chloride anion, taking on a five coordinate structure, which was also supported by the ESR signals observed at $g_{\perp}$ = 6 and $g_{//}$ = 2.0 due to the ferric high-spin-species (data not shown). Furthermore, the increase in the absorption coefficient for the Soret-band (400 nm) also supported that the aggregated form of heme can be converted to the isolated form in the presence of surfactants, SDS and lipids (*30*). The spectrum of heme in the supernatant in the absence of a peptide (spectrum 1 in Fig. 3) showed a broad Soret-band, with maxima at 360 and 385 nm, indicating that heme exists as a high-spin complex similar to that in membranes, but in an aggregated form. In contrast, after incubation of the heme-membrane complex with R27, the absorption of heme remaining in the membranes (spectrum 6 in Fig. 3) decreased, while that released into the supernatant significantly increased (spectrum 3 in Fig. 3). Moreover, spectrum 3 exhibited relatively sharp Soret- and Q-band absorption maxima at 413 nm, and 533 nm and 564 nm, respectively, which is similar to in the case of a six coordinate complex having strong ligands at both axial positions of heme. These results demonstrate that R27 binds to heme through the nitrogenous donors of imidazole groups of histidine residues, and is able to remove about 50% of membrane-bound heme from membranes. In contrast, the absorption spectra did not change on incubation of the heme-membrane complex with R18, as shown by spectra 2 and 5 in Fig. 3, indicating that R18 can not remove heme from the bound membranes.

Compared to the affinity of PfHRP2 for heme (K_d = 0.94 μM) (*31*), the affinity of R18 (2.21 μM) for heme is two-fold weaker, but the affinity of R27 for heme (0.71 μM) is slightly greater under these experimental conditions. We suggest that the affinity of R27 for heme might be high as that of PfHRP2, and is high enough to enable R27 to remove heme from membrane-intercalated heme. Based on these results and the fact that R27 exhibits much higher affinity to heme, we could explain why R27 inhibits heme-dependent hemolysis more strongly than R18 does.

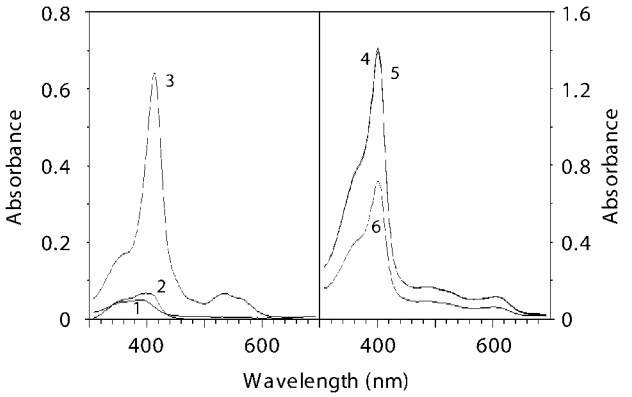

Fig. 3. **Removing heme from heme-bound membrane with peptides.** Heme-bound membranes were incubated in the presence or absence of a peptide, and then the absorption spectra of supernatants and pellets containing heme were recorded after incubation with 50 mM Tris-HCl and 2.5% SDS, pH 7.4. The absorption spectra of supernatants after incubation without a peptide (1), or with 20 μM R18 (2) or 20 μM R27 (3) are shown in the left panel. The absorption spectra of pellets after incubation without a peptide (4), or with 20 μM R18 (5) or 20 μM R27 (6) are shown in the right panel.

PfHRP2 has been reported to initiate the polymerization of heme in malarial food vacuoles (*15*), and to promote the H_2O_2-induced degradation of heme at pH 5.2 in food vacuoles (*9*). We suggest that PfHRP2 may play an important role in the neutralization of toxic heme in the parasite cytoplasm and infected erythrocytes by removing heme from heme-bound membranes, chelating heme in the cytosol, and reducing heme-induced hemolysis. Some studies argue against the role of PfHRP2 in hemozoin formation because of the existence of a parasite clone, 3B-D5, that lacks both PfHRP2 and PfHRP3, but still forms hemozoin (*32*). However, many histidine-rich proteins such as PfHRP4 have been suggested to be possible candidates for the detoxification of heme (*15*, *33*).

REFERENCES

1. Trigg, P.I. and Kondrachine, A.V. (1998) *Malaria: Parasite Biology*, *Pathogenesis*, *and Protection* (Irwin W. Sherman, ed.) pp. 11–22, ASM Press, Washington, DC
2. Inselburg, J. (1985) Induction and isolation of artemisinine-resistant mutants of *Plasmodium falciparum*. *Am. Soc. Trop. Med. Hyg.* **34**, 417–418
3. Chou, A.C. and Fitch, C.D. (1980) Hemolysis of mouse erythrocytes by ferriprotoporphyrin IX and chloroquine. Chemotherapeutic implications. *J. Clin. Invest.* **66**, 856–858
4. Kirschcner-Zilber, I., Rabizadeh, E., and Shaklai, N. (1982) The interaction of hemin and bilirubin with the human red cell membrane. *Biochim. Biophys Acta* **690**, 20–30
5. Menting, J.G., Tilley, L., Deady, L.W., Ng, K., Simpson, R.J., Cowman, A.F., and Foley, M. (1997) The antimalarial drug, chloroquine, interacts with lactate dehydrogenase from *Plasmodium falciparum*. *Mol. Biochem. Parasitol.* **88**, 215–224
6. Ahmad, H., Singh, S.V., and Awasthi, Y.C. (1991) Inhibition of bovine lens glutathione S-transferases by hematin, bilirubin, and bromosulfophthalein. *Lens Eye Toxic Res.* **8**, 431–440
7. Francis, S.E., Sullivan, D.J., and Goldberg, D.E. (1997) Hemoglobin metabolism in the malaria parasite *Plasmodium falciparum*. *Annu. Rev. Microbiol.* **51**, 97–123

8. Loria, P., Miller, S., Foley, M., and Tilley, L. (1999) Inhibition of the peroxidative degradation of haem as the basis of action of chloroquine and other quinoline antimalarials. *Biochem. J.* **339**, 363–370
9. Papalexis, V., Siomos, M.A., Campanale, N., Guo. X., Kocak, G., Foley. M., and Tilley, L. (2001) Histidine-rich protein 2 of the malaria parasite, *Plasmodium falciparum*, is involved in detoxification of the by-products of haemoglobin degradation. *Mol. Biochem. Parasitol.* **115**, 77–86
10. Atamna, H. and Ginsburg, H. (1995) Heme degradation in the presence of glutathione. A proposed mechanism to account for the high levels of non-heme iron found in the membranes of hemoglobinopathic red blood cells. *J. Biol. Chem.* **270**, 24876–24883
11. Ginsburg, H., Famin, O., Zhang, J., and Krugliak, M. (1998) Inhibition of glutathione-dependent degradation of heme by chloroquine and amodiaquine as a possible basis for their antimalarial mode of action. *Biochem. Pharmacol.* **56**, 1305–1313
12. Platel, D.F.N., Mangou, F., and Tribouley-Duret, J. (1999) Role of glutathione in the detoxification of ferriprotoporphyrin IX in chloroquine resistant *Plasmodium berghei*. *Mol. Biochem. Parasito.* **98**, 215–223
13. Wellems, T.E. and Howard, R.J. (1986) Homologous genes encode two distinct histidine-rich proteins in a cloned isolate of *Plasmodium falciparum*. *Proc. Natl Acad. Sci. USA* **83**, 6065–6069
14. Howard, R.J., Uni, S., Aikawa, M., Aley, S.B., Leech, J.H., Lew, A.M., Wellems, T.W., Rener, J., and Taylor, D.W. (1986) Secretion of a malarial histidine-rich protein (Pf HRP II) from *Plasmodium falciparum*-infected erythrocytes. *J. Cell Biol.* **103**, 1269–1277
15. Sullivan, J.D.J., Gluzman, I.Y., and Goldberg, D.E. (1996) *Plasmodium* hemozoin formation mediated by histidine-rich proteins. *Science* **271**, 219–222
16. Shaklai, N., Shviro, Y., Rabizadeh, E., and Kirschner-Zilber, I. (1985) Accumulation and drainage of hemin in the red cell membrane. *Biochim. Biophys Acta* **821**, 355–366
17. Huy, N.T., Kamei, K., Yamamoto, T., Kondo, Y., Kanaori, K., Takano, R., Tajima, K., and Hara, S. (2002) Clotrimazole binds to heme and enhances heme-dependent hemolysis: proposed antimalarial mechanism of clotrimazole. *J. Biol. Chem.* **277**, 4152–4158
18. Hulme, E.C. (1992) *Receptor-Ligand Interactions: A Practical approach*, Oxford University Press, New York
19. Chou, A.C., Chevli, R., and Fitch, C.D. (1980) Ferriprotoporphyrin IX fulfills the criteria for identification as the chloroquine receptor of malaria parasites. *Biochemistry* **19**, 1543–1549
20. Fitch, C.D., Chevli, R., and Gonzalez, Y. (1974) Chloroquine-resistant *Plasmodium falciparum*: effect of substrate on chloroquine and amodiaquin accumulation. *Antimicrob. Agents Chemother.* **6**, 757–762
21. Shviro, Y. and Shaklai, N. (1987) Glutathione as a scavenger of free hemin. A mechanism of preventing red cell membrane damage. *Biochem. Pharmac.* **36**, 3801–3807
22. Kaminsky, L.S., Byrne, M., and Davison, A.J. (1972) Iron ligands in different forms of ferricytochrome *c*: the 620-nm band as a probe. *Arch. Biochem. Biophys.* **150**, 355–361
23. Pasternack, R.F., Gillies, B.S., and Stahlbush, J.R. (1978) Kinetics and thermodynamics of the reactions of two iron (III) porphyrins with imidazole and 1-methylimidazole in dimethyl sulfoxide. *J. Amer. Chem. Soc.* **100**, 2613–2619
24. Babcock, G.T., Widger, W.R., Cramer, W.A., Oerling, W.A., and Metz, J.G. (1985) Axial ligands of chloroplast cytochrome b-559: identification and requirement for a heme-cross-linked polypeptide structure. *Biochemistry* **24**, 3638–3645
25. Choi, C.Y.H., Cerda, J.F., Chu, H.A., Babcock, G.T., and Marletta, M.A. (1999) Spectroscopic characterization of the heme-binding sites in *Plasmodium falciparum* histidine-rich protein 2. *Biochemistry* **38**, 16916–16924
26. Momenteau, M. (1973) The physical chemistry of hemes and hemopeptides. I. Physiochemical properties and reduction of chlorodeuterohemin in organic solvent. *Biochim. Biophys Acta* **304**, 814–827
27. Bohan, T.L. (1977) Analysis of low-spin ESR spectra of ferric heme proteins: a reexamination. *J. Magn. Reson.* **26**, 109–118
28. Beaven, G.H., Chen, S., D'Albis, A., and Gratm, W.B. (1974) A spectroscopic study of the haemin–human-serum-albumin system. *Eur. J. Biochem.* **41**, 539–546
29. Lovstad, R.A. (1986) Hemin-induced lysis of rat erythrocytes. Protective action of ceruloplasmin and different serum albumins. *Int. J. Biochem.* **18**, 171–173
30. Tajima, K., Ishikawa, Y., Mukai, K., Ishizu, K., and Sakurai, H. (1984) Optical and ESR studies on the micellar formation with surfactant Cu(II)-porphyrin. *Bull. Chem. Soc. Jpn.* **57**, 3587–3588
31. Pandey, A.V., Bisht, H., Babbarwal, V.K., Srivastava, J., Pandey, K.C., and Chauhan, V.S. (2001) Mechanism of malarial haem detoxification inhibition by chloroquine. *Biochem. J.* **355(Pt 2)**, 333–338
32. Wellems, T.E., Walker-Jonah, A., and Panton, L.J. (1991) Genetic mapping of the chloroquine-resistance locus on *Plasmodium falciparum* chromosome 7. *Proc. Natl Acad. Sci. USA* **88**, 3382–3386
33. Lenstra, R., d'Auriol, L., Andrieu, B., Le Bras, J., and Galibert, F. (1987) Cloning and sequencing of *Plasmodium falciparum* DNA fragments containing repetitive regions potentially coding for histidine-rich proteins: identification of two overlapping reading frames. *Biochem. Biophys. Res. Commun.* **146**, 368–377